NJC

Accepted Manuscript

This is an *Accepted Manuscript*, which has been through the Royal Society of Chemistry peer review process and has been accepted for publication.

Accepted Manuscripts are published online shortly after acceptance, before technical editing, formatting and proof reading. Using this free service, authors can make their results available to the community, in citable form, before we publish the edited article. We will replace this *Accepted Manuscript* with the edited and formatted *Advance Article* as soon as it is available.

You can find more information about *Accepted Manuscripts* in the Information for Authors.

Please note that technical editing may introduce minor changes to the text and/or graphics, which may alter content. The journal's standard Terms & Conditions and the Ethical guidelines still apply. In no event shall the Royal Society of Chemistry be held responsible for any errors or omissions in this *Accepted Manuscript* or any consequences arising from the use of any information it contains.

ROYAL SOCIETY OF CHEMISTRY

www.rsc.org/njc

Journal Name

RSCPublishing

ARTICLE

Rational design of organoboron heteroarene derivatives as luminescent and charge transport materials for organic light-emitting diodes

Cite this: DOI: 10.1039/x0xx00000x

Ruifa Jin* and Wenmin Xiao

Received 00th January 2012,
Accepted 00th January 2012

DOI: 10.1039/x0xx00000x

www.rsc.org/

A series of organoboron heteroarene derivatives has been designed for applications in organic light-emitting diodes (OLEDs). Their optical, electronic, and charge transport properties have been explored theoretically by using density functional theory (DFT) and time-dependent DFT (TD-DFT). The frontier molecular orbitals (FMOs) and local density of states analysis have turned out that the vertical electronic transitions of absorption and emission are characterized as intramolecular charge transfer (ICT). The calculated results show that their optical, electronic, and charge transport properties are affected by the different heteroaromatic groups. Our results reveal that the molecules under investigation can serve as luminescent materials for OLEDs. In addition, molecules under investigation are expected to be promising candidates for hole and/or electron transport materials. We have also predicted the mobility of the studied compounds. On the basis of investigated results, we proposed a rational way for the design of luminescent materials as well as charge transport materials simultaneously for OLEDs.

Introduction

Four-coordinate organoboron compounds have recently stirred great attention in connection with their broad applications in optoelectronic devices, such as emitters, electron-transport materials, host/hole blocking materials for organic light-emitting diodes (OLEDs), probes, sensors, and photoresponsive materials.[1–7] Especially, boron-containing aromatic and conjugated heterocycles appear to be particularly attractive for use in OLEDs owing to their high thermal and chemical stability.[8–10] However, the lower efficiency of OLEDs is still the main obstacle for their commercialization application. The intense luminescence and high carrier mobility of materials are the two most important parameters for high performance OLEDs.[11] Therefore, it has become one of the urgent research topics for the research community to develop new high efficiency multifunctional organic materials that exhibit carrier mobility for use in OLEDs. Four-coordinate organoboron compounds represent a promising class of multifunctional materials for OLEDs. This type of molecular structure has become the most efficient strategy used in the design and synthesis of OLEDs materials with the tunable properties. Four-coordinate organoboron compounds containing a π-conjugated organic backbone attached to a tetrahedral boron center display pronounced charge-transport properties and strong fluorescence with high quantum yields. The chelate ligands with rich π-electrons are coordinated with boron center with empty π-orbitals to allow intramolecular electron delocalization and the formation of rigid π-conjugated skeletons. The π-conjugated framework of four-coordinate organoboron compounds intensify the emission and enhance the electron-transport properties.[12,13] Theoretical study provides an essential role in developing materials. A number of studies demonstrate the interplay between theory and experiment, which is capable of providing useful insights to the understanding of the nature of molecules.[14–16] Recently, some four-coordinate organoboron compounds have been reported.[17] It was found that these molecules have large Stokes shift, high fluorescence quantum yield, and excellent photostability properties.

In this work, we report the investigation of both optical and charge transporting properties from theoretical point of view for four-coordinate organoboron derivatives. The purpose of this molecular architecture was to investigate the relationship between topologic structure and optical as well as electronic properties, rendering it a good candidate for OLEDs materials. Several derivatives (Scheme 1) have been designed to provide a demonstration for the rational design of novel luminescent and charge transporting materials for OLEDs. We also investigated their carrier mobility property of the compounds under investigation.

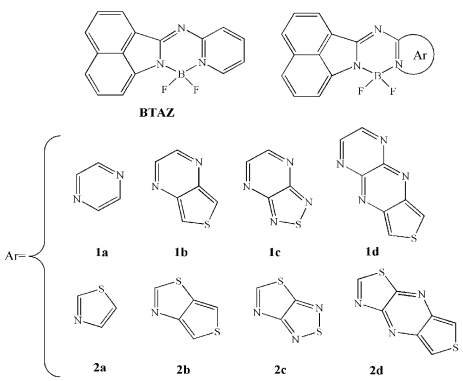

Scheme 1 Molecular structures of the investigated molecules

Computational methods

All calculations were carried out with the aid of the Gaussian 09 package.[18] The equilibrium structures of the compounds under investigation in ground states (S_0) were optimized using the B3LYP method. The corresponding structures in the first excited singlet state (S_1) were optimized using TD-B3LYP. All geometry optimizations were performed using the 6-31G(d,p) basis set. The harmonic vibrational frequency calculations using the same methods as for the geometry optimizations were used to ascertain the presence of a local minimum. Absorption and fluorescent properties of the studied compounds were predicted using the TD-B3LYP/6-31+G(d,p) based on the optimized S_0 and S_1 geometries, respectively.

According Marcus' "hopping" mechanism,[19,20] the charge transfer rate can be calculated by means of the following equation:

$$K = (V^2/\hbar)\left(\pi/\lambda k_B T\right)^{1/2} \exp\left(-\lambda/4k_B T\right) \quad (1)$$

where k_B is the Boltzmann constant and T is the absolute temperature. λ and V correspond to the reorganization energy and the charge transfer integral, respectively. From eq 1, one can find that the λ and V are the two key parameters.

For the reorganization energy λ, they consist of contributions from the external reorganization energy (λ_{ext}) and internal reorganization energy (λ_{int}). λ_{ext} represents the effect of polarized medium on charge transfer. λ_{int} means a measure of structural change between ionic and neutral states.[21] The computed values of the λ_{ext} in pure organic condensed phases are not only small but also are much smaller than their λ_{int}.[22–24] Moreover, there is a clear correlation between λ_{int} and charge transfer rate in literature.[25,26] Therefore, we focus on the λ_{int} exclusively. The λ_e and λ_h can be calculated by equations (2) and (3):[27]

$$\lambda_e = \left(E_0^- - E_-^-\right) + \left(E_-^0 - E_0^0\right) \quad (2)$$

$$\lambda_h = \left(E_0^+ - E_+^+\right) + \left(E_+^0 - E_0^0\right) \quad (3)$$

Where E_0^+ and E_0^- are the energy of the cation and anion calculated with the optimized structure of the neutral molecule, E_+^+ and E_-^- are the energy of the cation and anion calculated with the optimized cation and anion structure, and E_+^0 and E_-^0 are the energy of the neutral molecule calculated at the cationic and anionic state. Finally, E_0^0 is the energy of the neutral molecule in ground state. For comparing with the interested results reported previously,[28,29] the reorganization energies for electron (λ_e) and hole (λ_h) of the molecules were predicted at the B3LYP/6-31G(d,p) level on the basis of the single point energy.

The charge transfer integral for hole (electron) transfer can be obtained through a direct approach, which can be written:[30,31]

$$V_{ij} = \left\langle \phi_1^0 \middle| \hat{F}^0 \middle| \phi_2^0 \right\rangle \quad (4)$$

Here V_{ij} is the transfer integral, ϕ_1^0 and ϕ_2^0 are the unperturbed frontier orbital of molecules 1 and 2, respectively. $\hat{F}^0$ represents the Kohn–Sham–Fock operator of the dimer obtained with the unperturbed density matrix. $\hat{F}^0$ can be calculated by the molecular orbitals and density matrix of the two individual molecules, which can be studied separately by using the standard self-consistent field procedure. The pw91pw91/6-31G(d) method is employed to calculate the transfer integral. This method gave reasonable description for intermolecular coupling term previously.[32,33] In this work, for the crystal structures of the designed compounds are not available, we theoretically predict the crystal structures to calculate the transfer integrals. Molecular mechanics simulations have been used to optimize their conformations and crystal packings.[34] The crystal parameters have been successfully regenerated by molecular dynamics simulation.[35,36] Furthermore, it is reported in the literature that this method have been used to predict the crystal structures.[14,37,38] Therefore, the molecular crystal structures are predicted by the module Polymorph of software package Materials Studio.[39] The geometry of the cluster models used in present study was taken from B3LYP/6-31G(d,p) level.

The drift mobility of hopping, μ, can be evaluated from the Einstein equation:

$$\mu = \frac{e}{k_B T} D \quad (5)$$

Where e is the electronic charge, D is the diffusion coefficient, which can be evaluated as:[40]

$$D = \lim_{t\to\infty} \frac{1}{2n} \frac{\left\langle x(t)^2 \right\rangle}{t} \approx \frac{1}{2n} \sum_i d_i^2 k_i p_i = \frac{1}{2n} \frac{\sum_i d_i^2 k_i^2}{\sum_i k_i} \quad (6)$$

Here d_i is the center mass distance to neighbour i, n means the spatial dimension of the crystal, k_i is the hopping rate due to charge transfer to ith neighbour. P_i represents the relative probability for charge transfer to a particular ith neighbour, i.e.

$$P_i = \frac{k_i}{\sum_j k_i} \quad (7)$$

Results and discussion

Frontier molecular orbitals

To characterize the optical and electronic properties, it is useful to examine the frontier molecular orbitals (FMOs) of the compounds under investigation. The distribution patterns of the FMOs including the highest occupied molecular orbital (HOMO) and the lowest unoccupied molecular orbital (LUMO) of the studied compounds (**1a**–**1d** and **2a**–**2d**) are plotted in Fig. 1. The total and partial densities of states (TDOS and PDOS) on each fragment of the investigated molecules around the HOMO–LUMO gaps were calculated based on the current level of theory. The contributions of individual fragments (in %) to the FMOs of the studied compounds are given in Table 1. In all cases, both the HOMOs and LUMOs show π characteristics as visualized in Fig. 1. The $S_0 \rightarrow S_1$ excitation process can be mainly assigned to the HOMOs → LUMOs transitions, which corresponds to a π-π* excited singlet state. One can find that the HOMOs and LUMOs are spread over the whole conjugated molecule. It implies that the spatial overlap between the HOMOs and LUMOs are strong, which may result in stronger optical absorption corresponding to the transition from HOMOs to LUMOs. Furthermore, the distribution patterns of HOMOs and LUMOs also provide a remarkable signature for the charge-transfer character of the vertical $S_0 \rightarrow S_1$ transition. The results displayed in Table 1 show that the contributions of 2-difluoro-1,3,5,2-triazaborinine (FTRB) and heteroaromatic groups (HAR) fragments for **1a**–**1d** to LUMOs are increased, while the corresponding contributions of naphthalene (NA) fragments are decreased compared with those of to HOMOs, respectively. However, for **2a**–**2d**, the contributions of NA and FTRB fragments to LUMOs are increased, while the corresponding contributions of HAR fragments are decreased compared with those of to HOMOs, respectively. It indicates that the excitation of the electron from the HOMOs to LUMOs leads the electronic density to flow mainly from the NA fragments to FTRB and HAR fragments for **1a**–**1d**, while the corresponding electronic density to flow mainly from HAR fragments to NA and FTRB fragments for **2a**–**2d**. The percentages

of charge transfer are the differences between the contributions of fragments for LUMOs and the corresponding contributions for HOMOs in the compounds under investigation. The percentages of charge transfer from NA fragments to FTRB and HAR fragments are 8.2 ~ 24.6% for **1a**–**1d**. The corresponding percentages of charge transfer from the HAR fragments to NA and FTRB fragments are 7.9 ~ 16.3% for **2a**–**2d**. The results displayed in Table 1 reveal that the NA fragments serve as donors and FTRB and HAR fragments serve as acceptors for **1a**–**1d**. The HAR fragments serve as donors and NA and FTRB fragments serve as acceptors **2a**–**2d**. Furthermore, the photophysical properties of intramolecular charge transfer are well known and highly dependent on the electron donor/acceptor strength.[41,42] The introduction of different donor (acceptor) groups strengthens the electron-donating (-withdrawing) abilities of donors (acceptors). Therefore, the ICT transition in such ring-fused structures become much easier after introducing of different donor (acceptor) groups, resulting in the large bathochromic shift in their absorption and fluorescence spectra.

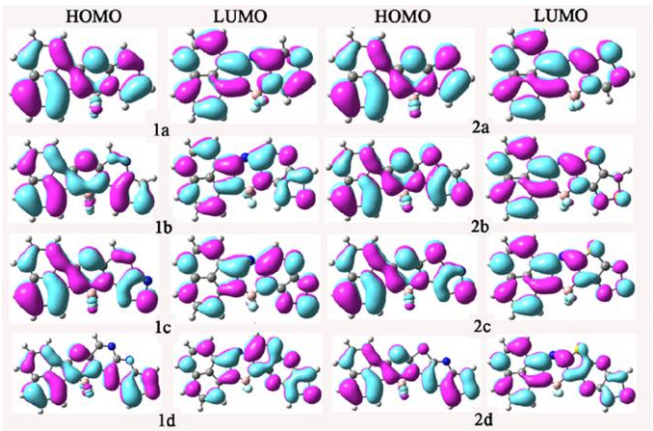

Fig. 1 The electronic density contours of the frontier orbitals for **1a**–**1d** and **2a**–**2d** at the B3LYP/6-31G(d,p) level

Table 1 The contributions of individual fragments (in %) to the FMOs of the studied compounds at the B3LYP/6-31G(d,p) level

	HOMOs			LUMOs		
Species	NA[a]	FTRB[b]	HAR[c]	NA[a]	FTRB[b]	HAR[c]
BATZ	51.6	33.9	14.5	52.4	35.5	12.4
1a	52.9	32.8	14.3	44.7	38.8	16.4
1b	45.0	34.3	20.7	34.6	38.2	27.2
1c	50.5	33.1	16.4	25.9	35.2	38.9
1d	33.1	28.9	37.9	21.0	29.6	49.4
2a	46.9	33.4	19.7	56.6	34.9	8.5
2b	43.0	32.5	24.5	55.3	36.5	8.2
2c	48.0	30.5	21.5	50.1	37.3	12.5
2d	37.5	29.0	33.5	41.4	33.0	25.6

[a]NA: Naphthalene fragment; [b]FTRB: 2-difluoro-1,3,5,2-triazaborinine fragment; [c]HAR: heteroaromatic groups.

It is well-known that the HOMO energy (E_{HOMO}), LUMO energy (E_{LUMO}), and HOMO–LUMO energy gap (E_g) are heavily related to the optical and electronic properties. To understand the influence of the optical and electronic properties, the E_{HOMO}, E_{LUMO}, and E_g values of the studied compounds were calculated and the results are summarized in Table 1. One can find that both the E_{HOMO} and E_{LUMO} values of the studied compounds decrease compared with those of parent compound chelate boron-containing 1,3,5-triazine derivative (**BTAZ**, see Scheme 1), as shown in Table 1. The E_{HOMO} values are in the order of **BTAZ** > **2a** > **1a** > **2b** > **1b** > **1d** > **2d** > **2c** > **1c**. The sequence of E_{LUMO} is **BTAZ** > **2a** > **2b** > **1a** > **2b** > **2d** > **2c** > **1d** > **1c**. Thus, the E_g values are in the order of **BTAZ** > **2a** ≈ **2b** > **2c** > **1a** > **2d** > **1b** > **1c** > **1d**. It suggests that the E_g values of the molecules with pyrazine fragments are smaller than that of the corresponding molecules with thiazole fragments. Furthermore, for both molecules with pyrazine and thiazole fragments, the E_g values decrease by introduction of thiophene, 1,2,5-thiadiazole, and thieno[3,4-b]pyrazine functional groups on pyrazine or thiazole rings, respectively. It suggests that the E_g values are affected by the introduction of different heteroaromatic groups to these molecules.

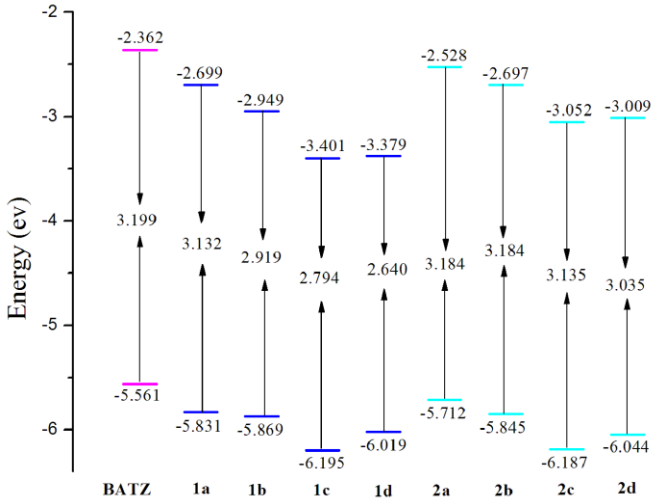

Fig. 2 The FMOs Energies E_{HOMO} and E_{LUMO} and HOMO–LUMO gaps E_g (all in eV) of the studied compounds at the B3LYP/6-31G(d,p) level

Absorption and fluorescence spectra

The absorption λ_{abs} and fluorescence λ_{fl} wavelengths, main assignments, and the oscillator strength f for the most relevant singlet excited states of the compounds under investigation are listed in Tables 2 and 3, respectively. The λ_{abs} and λ_{fl} values of **BTAZ** are all in agreement with experimental results,[17] the deviations are 2 and 31 nm, respectively. The Stokes shift of **BTAZ** is 113 nm, which is comparable to the experimental 80 nm. Thus, this result credits to the computational approach, so appropriate electronic transition energies can be predicted at these levels for this kind of system.

For the absorption spectra, the HOMOs → LUMOs transitions play a dominant role for the compounds under investigation. The results presented in Table 2 show that the λ_{abs} of **1a**–**1d** and **2b**–**2d** have bathochromic shifts 7, 38, 51, 110, 8, 11, and 27 nm compared with that of the parent compound **BTAZ**, respectively. The λ_{abs} of **2a** is almost equal to that of **BTAZ**. Moreover, **1b**, **1c**, **2b**, and **2c** have larger oscillator strengths than that of **BTAZ**. The f value **1a**, **2a**, and **2d** are almost equal to that of **BTAZ**, while the corresponding value of **1d** is slightly less than of **BTAZ**. The oscillator strength for an electronic transition is proportional to the transition moment.[43] In general, larger oscillator strength corresponds to larger experimental absorption coefficient or stronger fluorescence intensity. This indicates that the compounds under investigation shown larger absorption intensity than that of **BTAZ** except for **1d**.

For the fluorescence spectra, the LUMOs ← HOMOs excitations play a dominant role for **BTAZ**, **1a**, **1c**, and **2a**–**2c** while the fluorescence of **1b**, **1d**, and **2d** mainly arise from HOMOs-1 ← LUMOs excitations. As shown in Table 3, the λ_{fl} values of **1a**–**1c** and **2a**–**2c** show bathochromic shift 1, 13, 41, 4, 8, and 19 nm compared with that of **BTAZ**, respectively. The Stokes shifts of **1a**–**1c** and **2a**–**2c** are 107, 88, 103, 118, 114, and 121 nm, respectively. The λ_{fl} of **1d** and **2d** have hypsochromic shifts 13 and 34 nm

compared with that of **BTAZ**, respectively. Furthermore, the *f* values of the compounds under investigation are larger than that of **BTAZ** except that the corresponding value of **2a** is almost equal to that of **BTAZ**, corresponding to strong fluorescence spectra. This implies that the studied compounds have large fluorescent intensity and they are promising luminescent materials for OLEDs.

Table 2 The longest wavelength of absorption spectrum λ_{abs}, corresponding oscillator strength *f*, and assignments (coefficient) for the compounds under investigation at the TD-B3LYP/6-31+G(d,p)//B3LYP/6-31G(d,p) level, along with available experimental data

Species	λ_{abs}	*f*	Assignment
BTAZ	436	0.42	H → L (69%)
1a	443	0.41	H → L (70%)
1b	474	0.48	H → L (70%)
1c	487	0.53	H→L (70%)
1d	546	0.10	H→L (62%)
2a	435	0.40	H→L (69%)
2b	444	0.51	H→L (70%)
2c	447	0.50	H→L (69%)
2d	463	0.43	H→L (68%)
EXP[a]	438		

[a] The Experimental λ_{abs} of **BTAZ** in CH_2Cl_2 were taken from Ref. [17].

Table 3 The strongest fluorescence wavelengths λ_{fl} (in nm), the oscillator strength *f*, and main assignments (coefficient) of the compounds under investigation at the TD-B3LYP/6-31+G(d,p)//TD-B3LYP/6-31(d,p) level, along with available experimental data

Species	λ_{fl}	*f*	Assignment
BTAZ	549	0.26	H←L (69%)
1a	550	0.27	H←L (69%)
1b	562	0.41	H-1←L (70%)
1c	590	0.44	H←L (70%)
1d	538	0.64	H-1←L (68%)
2a	553	0.24	H←L (69%)
2b	558	0.30	H←L (69%)
2c	568	0.28	H←L (69%)
2d	515	0.57	H-1←L (69%)
EXP[a]	518		

[a] The Experimental λ_{fl} of **BTAZ** in CH_2Cl_2 were taken from Ref. [17].

Reorganization energy

The calculated reorganization energies for hole and electron are listed in Table 4. It is well-known that, the lower the reorganization energy values, the higher the charge transfer rate.[19,20] The results displayed in Table 4 show that the λ_h values of the compounds under investigation (0.197 – 0.279 eV) are smaller than that of N,N'-diphenyl-N,N'-bis(3-methlphenyl)-(1,1'-biphenyl)-4,4'-diamine (TPD), which is a typical hole transport material (λ_h = 0.290 eV).[28] It indicates that the hole transfer rates of the compounds under investigation may be higher than that of TPD. On the other hand, the calculated λ_e values of **1a**–**1d**, **2c**, and **2d** are smaller than that of tris(8-hydroxyquinolinato)aluminum(III) (Alq3) (λ_e = 0.276 eV), a typical electron transport material.[29] It suggests that the electron transfer rates of **1a**–**1d**, **2c**, and **2d** might be higher than that of Alq3. However, the λ_e values of **2a** and **2b** are larger than that of Alq3, indicating that the electron transfer rates of **2a** and **2b** might be lower than that of Alq3. It suggests that the electron transfer rates of **2a** and **2b** might be lower than that of Alq3. Therefore, these molecules are potential electron and hole transport materials except **2a** and **2b** can serve as hole transport materials only under the proper operating conditions for OLEDs from the stand point of the smaller reorganization energy. The λ_h values are predicted in the order **1d** < **1b** < **1a** < **1c** for **1a**–**1d** and **2b** < **2d** < **2a** < **2c** for **2a**–**2d**, respectively. This shows that the instruction of thiophene and thieno[3,4-b]pyrazine fragments lead to the increase of hole transfer rates, while instruction of 1,2,5-thiadiazole fragments decrease the hole transfer rates for the compounds under investigation. For the λ_e, the prediction of λ_e values is in the sequence **1b** < **1d** < **1c** < **1a** for **1a**–**1d** and **2d** < **2c** < **2b** < **2a** for **2a**–**2d**, respectively. This shows that the introduction of the thiophene, 1,2,5-thiadiazole, and thieno[3,4-b]pyrazine fragments results in decrease of electron transfer rates for molecules under investigation.

Table 4 Calculated molecular λ_e and λ_h (in eV) of the compounds under investigation at the B3LYP/6-31G(d,p) level.

Species	λ_h	λ_e
1a	0.275	0.259
1b	0.214	0.197
1c	0.279	0.216
1d	0.198	0.200
2a	0.231	0.350
2b	0.197	0.333
2c	0.254	0.273
2d	0.199	0.192

Calculated crystal structure and transport properties

We calculated the mobility of the compounds under investigation to study their charge transport property. The calculated total energies of the compounds under investigation in different space groups are summarized in Table S1 in ESI. The lattice constants of the compounds under investigation with the lowest total energies are listed in Table S2 in ESI. We predict the mobility of the compounds under investigation with the lowest total energies. The transmission paths are selected according to the optimized crystal structures. We arbitrarily choose one molecule in the crystal as the carrier donor and take all its neighboring molecules as paired elements. Each pair is defined as a transmission path. Then the charge transfer integral can be calculated according to the transmission path. The mobility can be estimated from the Einstein relation. The predicted crystal structures of **1d** and **2d** as representation are shown in Fig. 3. The calculated crystal structures of **1d** and **2d** with the lowest total energies belong to $P2_12_12_1$ and *Pbca* space groups, respectively. Fig. 4 shows the most important pathways (dimers) for **1d** and **2d**. The calculated transfer integrals of **1d** and **2d** for holes and electrons in space groups $P2_12_12_1$ and *Pbca* respectively are listed in Table 5. We also calculated the charge transfer integrals of **1d** in *Cc* space group and **2d** in $Pna2_1$ space group and the results are summarized in Table S3 in ESI. The calculated holes and electrons transfer integrals and the corresponding space groups of **1a**–**1c** and **2a**–**2c** with the lowest total energies are listed in Table S4 in ESI. The data in Table 5 reveal that the electronic coupling is determined by the relative distance and orientations of the interacting molecules.[44] Furthermore, from Table 5, one can find that **1d** possesses the largest absolute electron and hole coupling values in pathways 5 and 6 for space group $P2_12_12_1$, respectively. For **2d**, it possesses the largest absolute electron and hole coupling values in pathway 5 for space group *Pbca* and in pathways 1 and 2 for space group $Pna2_1$. It indicates that the orientation of the interacting molecules is the key factor of hole or electron coupling values. The reason is that the co-facial stacking structure is expected to provide more efficient orbital overlap leading to the most efficient charge transfer route.[44] The calculated electron and hole mobility of the compounds under investigation are listed in the Table 6. The results displayed in Table 6 show that the hole mobility values of the compounds under investigation are larger than that of **TPD** (1.0×10^{-3} cm^2 V^{-1} s^{-1})[45] except the corresponding value of **1b** (4.43×10^{-4} cm^2 V^{-1} s^{-1}) is slightly smaller than that of **TPD**. The hole mobility values are in the order of **1c** > **1a** > **1d** > **1b**

for **1a**–**1d** and **2a** > **2c** > **2b** > **2d** for **2a**–**2d**. It suggests that the hole mobility values can be increased by introduction of the 1,2,5-thiadiazole group, while the introduction of thiophene and thieno[3,4-b]pyrazine groups leads to a decrease in the hole mobility values for the molecules with pyrazine fragments. The introduction of thiophene, 1,2,5-thiadiazole, and thieno[3,4-b]pyrazine groups leads to a decrease in the hole mobility values for the molecules with thiazole fragments. The sequences of electron mobility are **1a** > **1b** > **1d** > **1c** for **1a**–**1d** and **2d** > **2c** > **2a** > **2b** for **2a**–**2d**. One may conclude that the electron mobility values can be decreased by introduction of thiophene, 1,2,5-thiadiazole, and thieno[3,4-b]pyrazine groups for the molecules with pyrazine fragments. For the molecules with thiazole fragments, the introduction of 1,2,5-thiadiazole and thieno[3,4-b]pyrazine groups leads to a increase in the electron mobility values, while the introduction of thiophene group decreases the electron mobility value. In addition, both the values of electron and hole mobility for **1d** in $P2_12_12_1$ space group are larger than those in *Cc* space group, respectively. The values of electron and hole mobility for **2d** in *Pbca* space group are larger than those in $Pna2_1$ space group, respectively. Furthermore, the electron mobility values of **1d** and **2d** in two space groups are larger than those of hole mobility values, respectively. It shows that different space groups lead to different mobility values, that is to say, the stacking structure is the most important factor for molecular mobility property. The theoretical prediction shows that the compounds under investigation can be made as charge transfer materials using for OLEDs.

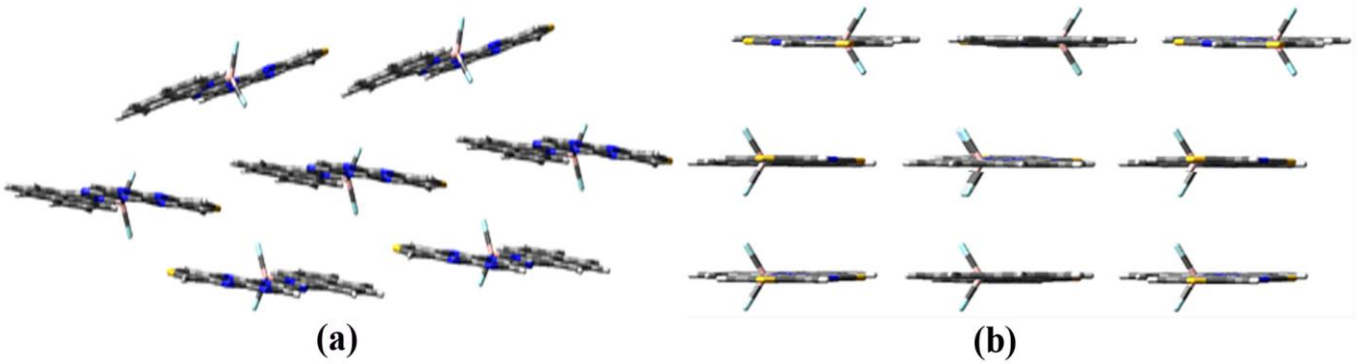

Fig. 3 Herringbone structures of **1d** in $P2_12_12_1$ space group (a) and **2d** in *Pbca* space group (b).

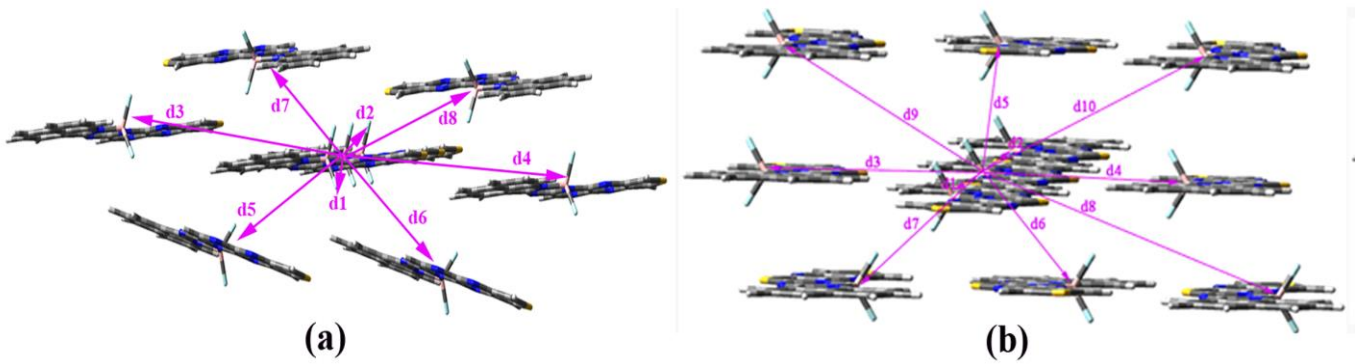

Fig. 4 Crystal structures and hopping routes of **1d** in $P2_12_12_1$ space group (a) and **2d** in *Pbca* space group (b).

Table 5 Center−center distance (in Å) and the corresponding hole and electron coupling (in eV) between the dimer in all of the nearest neighbor pathways for **1d** and **2d** in different space groups

Species	Space groups	Pathway	Distance	Electron coupling	Hole coupling
1d	$P2_12_12_1$	1	12.074	-3.60×10^{-6}	1.08×10^{-6}
		2	12.074	-3.60×10^{-6}	1.08×10^{-6}
		3	13.900	1.50×10^{-3}	-4.00×10^{-4}
		4	13.900	1.50×10^{-3}	-4.00×10^{-4}
		5	8.717	5.40×10^{-3}	2.40×10^{-3}
		6	11.042	1.95×10^{-4}	-2.50×10^{-3}
		7	9.819	1.40×10^{-3}	1.20×10^{-3}
		8	9.819	1.40×10^{-3}	1.20×10^{-3}
2d	*Pbca*	1	17.153	2.96×10^{-4}	-2.79×10^{-5}
		2	17.153	2.96×10^{-4}	-2.79×10^{-5}
		3	9.121	-3.47×10^{-6}	-5.89×10^{-5}
		4	9.121	-3.46×10^{-6}	-5.90×10^{-5}
		5	9.553	1.13×10^{-2}	-6.40×10^{-3}
		6	10.126	-2.80×10^{-3}	6.20×10^{-3}
		7	8.484	5.09×10^{-4}	2.96×10^{-4}
		8	13.179	-1.98×10^{-5}	-5.04×10^{-7}
		9	10.561	-8.03×10^{-5}	1.27×10^{-4}
		10	10.561	-8.05×10^{-5}	1.27×10^{-4}

Table 6 The electron and hole mobility of the compounds under investigation with the lowest total energies [T = 298.15 K, in $cm^2\ V^{-1}\ s^{-1}$]

Species	Space groups	Electron mobility	Hole mobility
1a	$P\bar{1}$	1.16×10^{-2}	3.30×10^{-2}
1b	$P2_1$	8.69×10^{-3}	4.43×10^{-4}
1c	$P2_1$	8.21×10^{-4}	5.70×10^{-2}
1d	$P2_12_12_1$	6.23×10^{-3}	1.80×10^{-3}
2a	*Cc*	7.01×10^{-4}	3.60×10^{-2}
2b	*Pbca*	2.49×10^{-4}	1.98×10^{-2}
2c	$Pna2_1$	1.03×10^{-2}	2.04×10^{-2}
2d	*Pbca*	4.22×10^{-2}	1.35×10^{-2}

Conclusions

In this paper, a series of four-coordinate organoboron derivatives have been systematically investigated for organic light-emitting diodes applications. The frontier molecular orbitals and local density of states analysis have turned out that the vertical electronic transitions of absorption and emission are characterized as intramolecular charge transfer (ICT). The calculated results show that their optical, electronic, and charge transport properties are affected by the aromatic groups. The frontier molecular orbitals energy gap (E_g) of molecules with pyrazine and thiazole fragments decrease by introduction of thiophene, 1,2,5-thiadiazole, and thieno[3,4-b]pyrazine groups on pyrazine or thiazole rings, respectively. The fluorescence wavelengths show bathochromic shift except the molecules with thieno[3,4-b]pyrazine groups (**1d** and **2d**) have hypsochromic shifts compared with that of parent compound chelate boron-containing 1,3,5-triazine derivative (**BTAZ)**. Furthermore, the studied compounds have large fluorescent intensity. Our results reveal that the molecules under investigation can serve as luminescent materials for organic light-emitting diodes. In addition, the reorganization energy results reveal that the studied compounds are expected to be promising candidates for electron and hole transport materials except molecules with thiazole and thiazo[3,4-d]thiazole fragments (**2a** and **2b**) can serve as hole transport materials only under the proper operating conditions. The charge mobility of the studied compounds were also investigated. The results show that the studied compounds have high hole and/or electron mobility. On the basis of investigated results, we proposed a rational way for the design of charge transport and luminescent materials for organic light-emitting diodes simultaneously.

Acknowledgements

Financial supports from the Research Program of Sciences at Universities of Inner Mongolia Autonomous Region (No. NJZZ235) and the Natural Science Foundation of Inner Mongolia Autonomous Region (No. 2015MS0201) are gratefully acknowledged.

Notes and references

Inner Mongolia Key Laboratory of Photoelectric Functional Materials and College of Chemistry and Chemical Engineering, Chifeng University, Chifeng 024000, China. Email: Ruifajin@163.com

† Electronic Supplementary Information (ESI) available: The total energies of the compounds under investigation in different space groups. The lattice constants of the compounds under investigation with the lowest total energies. The charge transfer integrals of **1d** in *Cc* space group and **2d** in *Pna2₁* space group. The calculated holes and electrons transfer integrals and the corresponding space groups of **1a**–**1c** and **2a**–**2c** with the lowest total energies. See DOI: 10.1039/b000000x/

1 Y. L. Rao, H. Amarne and S. Wang, *Coord. Chem. Rev.*, 2012, **256**, 759–770.
2 D. Li, H. Zhang and Y. Wang, *Chem. Soc. Rev.*, 2013, **42**, 8416–8433.
3 L. S. Huang and C. H. Chen, *Mater. Sci. Eng. R*, 2002, **39**, 143–222.
4 J. S. Lu, S. B. Ko, N. R. Walters, Y. Kang, F. Sauriol and S. Wang, *Angew. Chem. Int. Ed.*, 2013, **52**, 4544–4548.
5 Y. L. Rao, H. Amarne, L. C. Chen, N. Mosey and S. Wang, *J. Am. Chem. Soc.*, 2013, **135**, 3407–3410.
6 K. Ono, A. Nakashima, Y. Tsuji, T. Kinoshita, M. Tomura, J. I. Nishida and Y. Yamashita, *Chem.–Eur. J.*, 2010, **16**, 13539–13546.
7 B. L. Guennic, O. Maury and D. Jacquemin, *Phys. Chem. Chem. Phys.*, 2012, **14**, 157–164.
8 P. G. Campbell, A. J. V. Marwitz and S. Y. Liu, *Angew. Chem. Int. Ed.*, 2012, **51**, 6074 –6092.
9 A. Lorbach, A. Hübner and M. Wagner, *Dalton. Trans.*, 2012, **41**, 6048–6063.
10 A. J. Ashe III, *Organometallics*, 2009, **28**, 4236–4248.
11 C. Du, S. Ye, Y. Liu, Y. Guo, T. Wu, H. Liu, J. Zheng, C. Cheng, M. Zhuab and G. Yua, *Chem. Commun.*, 2010, **46**, 8573–8575.
12 Z. L. Zhang, H. Bi, Y. Zhang, D. D. Yao, H. Z. Gao, Y. Fan, H. Y. Zhang, Y. Wang, Y. P. Wang, Z. Y. Chen and D. G. Ma, *Inorg. Chem.*, 2009, **48**, 7230–7236.
13 H. Y. Zhang, C. Huo, J. Y. Zhang, P. Zhang, W. J. Tian and Y. Wang, *Chem. Commun.*, 2006, **3**, 281–283.
14 R. F. Jin and Y.F. Chang, *Phys. Chem. Chem. Phys.*, 2015, **17**, 2094–2103.
15 L. Y. Zou, Z. L. Zhang, A. M. Ren, X. Q. Ran and J. K. Feng, *Theor. Chem. Acc.*, 2010, **126**, 361–369.
16 R. F. Jin, *Theor. Chem. Acc.*, 2012, **131**, 1260–1270.
17 C. Cheng, N. Gao, C. Yu, Z. Wang, J. Wang, E. Hao, Y. Wei, X. Mu, Y. Tian, C. Ran and L. Jiao, *Org. Lett.*, 2015, **17**, 278−281.
18 M. J. Frisch, G. W. Trucks, H. B. Schlegel, G. E. Scuseria, M. A. Robb, J. R. Cheeseman, V. G. Zakrzewski, J. A. Montgomery, Jr., R. E. Stratmann, J. C. Burant, S. Dapprich, J. M. Millam, A. D. Daniels, K. N. Kudin, M. C. Strain, O. Farkas, J. Tomasi, V. Barone, M. Cossi, R. Cammi, B. Mennucci, C. Pomelli, C. Adamo, S. Clifford, J. Ochterski, G. A. Petersson, P. Y. Ayala, Q. Cui, K. Morokuma, D. K. Malick, A. D. Rabuck, K. Raghavachari, J. B. Foresman, J. Cioslowski, J. V. Ortiz, B. B. Stefanov, G. Liu, A. Liashenko, P. Piskorz, I. Komaromi, R. Gomperts, R. L. Martin, D. J. Fox, T. Keith, M. A. Al-Laham, C. Y. Peng, A. Nanayakkara, C. Gonzalez, M. Challacombe, P. M. W. Gill, B. G. Johnson, W. Chen, M. W. Wong, J. L. Andres, M. Head-Gordon, E. S. Replogle and J. A. Pople, *Gaussian 09*, Gaussian, Inc, Wallingford, CT2009.
19 R. A. Marcus, *Rev. Mod. Phys.*, 1993, **65**, 599−610.
20 R. A. Marcus, *Annu. Rev. Phys. Chem.*, 1964, **15**, 155−196.
21 V. Lemaur, M. Steel, D. Beljonne, J. L. Brédas and J. Cornil, *J. Am. Chem. Soc.*, 2005, **127**, 6077−6086.
22 D. L. Cheung and A. Troisi, *J. Phys. Chem. C*, 2010, **114**, 20479−20488.
23 N. G. Martinelli, J. Idé, R. S. Sánchez-Carrera, V. Coropceanu, J. L. Brédas, L. Ducasse, F. Castet, J. Cornil and D. Beljonne, *J. Phys. Chem. C*, 2010, **114**, 20678−20685.
24 D. P. McMahon and A. Trois, *J. Phys. Chem. Lett.*, 2010, **1**, 941−946.
25 M. E. Köse, H. Long, K. Kim, P. Graf and D. Ginley, *J. Phys. Chem. A*, 2010, **114**, 4388−4393.
26 K. Sakanoue, M. Motoda, M. Sugimoto and S. Sakaki, *J. Phys. Chem. A*, 1999, **103**, 5551−5556.
27 M. E. Köse, W. J. Mitchell, N. Kopidakis, C. H. Chang, S. E. Shaheen, K. Kim and G. Rumbles, *J. Am. Chem. Soc.*, 2007, **129**, 14257−14270.
28 B. C. Lin, C. P. Cheng, Z. Q. You and C. P. Hsu, *J. Am. Chem. Soc.*, 2005, **127**, 66−67.
29 N. E. Gruhn, D. A. da Silva Filho, T. G. Bill, M. Malagoli, V. Coropceanu, A. Kahn and J. L. Brédas, *J. Am. Chem. Soc.*, 2002, **124**, 7918−7919.
30 T. Fujita, H. Nakai and H. Nakatsuji, *J. Chem. Phys.*, 1996, **104**, 2410−2417.
31 A. Troisi and G. Orlandi, *J. Phys. Chem. A*, 2006, **110**, 4065−4070.
32 B. Liu, X. Chen, Y. Zou, L. Xiao, X. Xu, Y. He, L. Li and Y. Li, *Macromolecules*, 2012, **45**, 6898−6905.
33 Y. Geng, J. Wang, S. Wu, H. Li, F. Yu, G. Yang, H. Gao and Z. Su, *J. Mater. Chem.*, 2011, **21**, 134−143.
34 A. van Langevelde, P. Capkova, E. Sonneveld, H. Schenk, M. Trchova and M. Ilavsky, *J. Synchrotron. Rad.*, 1999, **6**, 1035–1043.
35 Y. H. Liu, Y. Xie and Z. Y. Lu, Chem. Phys., 2010, **367**, 160-166.
36 A. Irfan, J. P. Zhang and Y. F. Chang, *Theor. Chem. Acc.*, 2010, **127**, 587–594.
37 S. S. Tang and J. P. Zhang, *J. Phys. Chem. C* , 2013, **117**, 3221−3231.
38 S. S. Tang and J. P. Zhang, *J. Comput. Chem.*, 2012, **33**, 1353–1363.
39 Materials Studio; Accelrys Inc.: San Diego, CA, 2005.
40 W. Q. Deng and W. A. Goddard III, *J. Phys. Chem. B*, 2004, **108**, 8614−8621.
41 W. Huang, X. Zhang, L. Ma, C. Wang and Y. Jiang, *Chem. Phys. Lett.*, 2002, **352**, 401−407.

42 M. S. Alexiou, V. Tychopoulos, S. Ghorbanian, J. H. P. Tyman, R. G. Brown and P. I. Brittain, *J. Chem. Soc. Perkin. Trans.*, 1990, **2**, 837−842.
43 P. Schleyer, R. Von, N. L. Allinger, T. Clark, J. Gasteiger, P. A. Kollman, H. F. III Schaefer and P. R. Schreiners, Wiley, UK, Chichester, 1998.
44 C. L. Wang, F. H. Wang, X. D. Yang, Q. K. Li and Z. G. Shuai, *Org. Electron.*, 2008, **9**, 635−640.
45 K. Shizu, T. Sato, A. Ito, K. Tanaka and H. Kaji, *J. Mater. Chem.*, 2011, **21**, 6375−6382.

Graphic abstract:

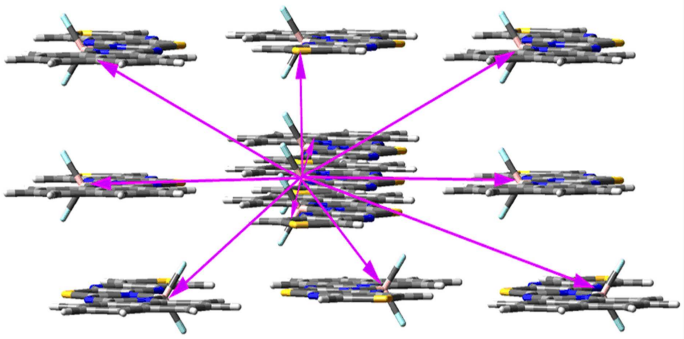

A series of organoboron heteroarene derivatives have been designed as luminescent and charge transport materials for OLEDs application.